Predictions of thermomagnetic properties of $HoAl_2$ and $ErAl_2$ performed with ATOMIC MATTERS MFA Computation System.

RAFAŁ MICHALSKI, JAKUB ZYGADŁO
INDUFORCE
M.Pszona 41/29 31-462 Cracow
POLAND
JAGIELLONIAN UNIVERSITY,
Faculty of Mathematics and Computer Science,
Łojasiewicza 6 30-348 Cracow,
POLAND
r.michalski@induforce.eu http://www.atomicmatters.eu

Abstract: We present the results of non-free parameter calculations of properties of $HoAl_2$ and $ErAl_2$ single crystals, performed with our new computation system called ATOMIC MATTERS MFA [1, 2]. A localized electron approach was applied to describe the electronic structure evolution of Ho and Er ions over a wide temperature range and estimate Magnetocaloric Effect (MCE). Thermomagnetic properties of $HoAl_2$ and $ErAl_2$ were calculated based on the fine electronic structure of the $4f^{10}$ and $4f^{11}$ electronic configuration of the Ho and Er ions, respectively. Our calculations yielded: magnetic moment value and direction; single-crystalline magnetization curves in zero field and in external magnetic field applied in various directions $\mathbf{m}(T,\mathbf{B}_{ext})$; the 4*f*-electronic components of specific heat $c_{4f}(T,\mathbf{B}_{ext})$; and temperature dependence of the magnetic entropy and isothermal entropy change with external magnetic field $-\Delta S(T,\mathbf{B}_{ext})$. The cubic universal CEF parameters values used for all CEF calculations was taken from [3] and recalculated for universal cubic parameters set for the RAl_2 series: A_4=+7.164Ka_0 and A_6 =-1.038Ka_0. Magnetic properties were found to be anisotropic due to cubic Laves phase C15 crystal structure symmetry. These studies reveal the importance of multipolar charge interactions when describing thermomagnetic properties of real 4*f* electronic systems and the effectiveness of an applied self-consistent molecular field in calculations for magnetic phase transition simulation.

Key-Words: - $HoAl_2$, $ErAl_2$, RAl_2, Laves Phase, CEF, MFA, MCE, Atomic Matters.

1 Introduction

Understanding and controlling the microscopic quantum mechanisms responsible for storing and releasing material entropy through controlled external magnetic field change processes is one of the biggest challenges in materials science. Our calculation methodology makes it possible to describe the thermomagnetic properties of magnetic materials, we decided to test our approach for $HoAl_2$ and $ErAl_2$ compounds. The material series RAl_2 compounds (R=Rare Earth) are intermetallic materials with interesting thermomagnetic properties [3]. In other words, the RAl_2 series of compounds are fascinating due to their large magnetocaloric entropy changes under external magnetic fields. This large change in MCE (Magnetocaloric Effect) is especially attractive in magnetic refrigeration due to its potential environmental friendliness compared to traditional gas refrigeration. We present the results of simulations of thermomagnetic properties of some RAl_2 compounds performed with our new computation system called ATOMIC MATTERS MFA [1,2]. A few calculation results for $HoAl_2$ compound are compared with experimental data taken from the literature [4-6] and for $ErAl_2$ from papers [7,8]. All the lanthanides combine with aluminum to form RAl_2 compounds with the same crystalline structure [3]. All RAl_2 compounds are ferromagnetic at low temperatures [3]. RAl_2 crystals have the so-called cubic Laves phase C15 structure, while the point symmetry for rare earth ions is $4^{-}3m$. The elementary cell of the crystal structure of Laves phase is presented in fig. 1. The CEF (Crystal Electric Field) parameters describing the multipolar charge interaction of R ions in the crystal surrounding in this structure was agreed for all compounds and established according to study of the $DyAl_2$ compound [3]for: A_4=+7.164Ka_0 and A_6 =-1.038Ka_0. We decided to predict the properties of $HoAl_2$ and $ErAl_2$ completely without free parameters; therefore, we used the established cubic CEF and molecular field factor n_{mol} that is recalculated from $DyAl_2$.

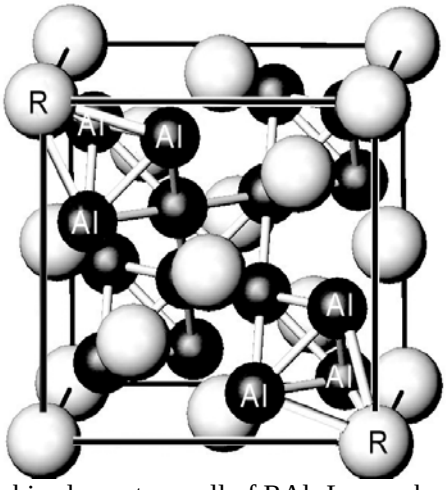

Fig.1. Cubic elementary cell of RAl_2 Laves phase C15 crystals.

2 Computation system

All calculations for $HoAl_2$ and $ErAl_2$ were performed with ATOMIC MATTERS MFA computation system. This is extension of the ATOMIC MATTERS application [1] describes fine electronic structure and predicts basic magnetic and spectral properties of materials in a paramagnetic state. ATOMIC MATTERS MFA computation system [2] provides magnetic, calorimetric and spectroscopic properties of atomic-like localized electron systems under the influence of Crystal Electric Field (CEF), spin-orbit coupling, and magnetic interactions, taken both as dynamic Mean Field Approximation (MFA), calculations and the influence of established external magnetic field $\mathbf{B}_{ext}$ [2]. ATOMIC MATTERS MFA provides macroscopic properties of materials in defined temperature regions, especially around the phase transition temperature: magnetic moment $\mathbf{m}(T,\mathbf{B}_{ext})$ (spin and orbital, directional components), localized electron specific heat $c_{4f}(T,\mathbf{B}_{ext})$, localized electron entropy with a useful tool set for MCE, isothermal entropy change $-\Delta S(T,\mathbf{B}_{ext})$ calculations, evolution of energy level positions, total free energy, and more.

To enhance their ease of use and efficacy, both calculation systems implement an advanced Graphic User Interface (GUI) with a system of hierarchical tabs for managing calculation results, 3D interactive visualizations of potentials and fields based on Open Graphics Library (OpenGL), intuitive tools, and databases. More up-to-date information about Atomic Matters computation systems are available on our web page [9].

3 Theoretical background

ATOMIC MATTERS MFA computation system calculation methodology is deeply rooted in atomic physics. Taking into consideration the individual population of states of fine electronic structure of ions/atoms at different temperatures according L. Boltzmann statistics makes it possible to define the temperature dependencies of single ionic properties. ATOMIC MATTERS MFA can simulate phase transitions of ionic/atomic systems according to dynamic calculations of the molecular field B_{mol}, simply defined as:

$$\mathbf{B}_{mol}(T) = n_{mol}\,\mathbf{m}(T) \qquad (1)$$

that interacts with ions to induce their magnetic moments. Such self-consistent calculations can only be performed after establishing the molecular field factor n_{mol} that is closely related to the temperature of phase transitions, T_C.

For rapid calculations in a thermodynamically stable temperature region, ATOMIC MATTERS offers the following CEF+Spin-Orbit+Zeeman Hamiltonian according to the chosen calculation space of ground multiplet $|J,Jz\rangle$ or ground atomic term $|LSL_zS_z\rangle$ respectively[1]:

$$H_J = H_{CEF} + H_{Zeeman} = \sum_n \sum_m B_n^m \hat{\mathbf{O}}_n^m(J, J_z) + g_L\,\mu_B\,\mathbf{J}\cdot\mathbf{B}_{ext} \qquad (2)$$

or

$$H_{LS} = H_{CEF} + H_{S\text{-}O} + H_{Zeeman} =$$

$$= \sum_n \sum_m B_n^m \hat{\mathbf{O}}_n^m(L, L_z) + \lambda\,\mathbf{L}\cdot\mathbf{S} + \mu_B(\mathbf{L} + g_e\,\mathbf{S})\cdot\mathbf{B}_{ext} \qquad (3)$$

For all Hamiltonians: B^m_n denotes CEF parameters, $\mathbf{O}^m_n$ are Stevens operators, λ-is the spin–orbit constant, and g_L and $g_e \approx 2.002319$ are the gyromagnetic factors of a whole ion or single electron respectively. For a whole ion or electron respectively, μ_B is the Bohr magneton and $\mathbf{B}_{ext}$ is the external magnetic field. In all cases, calculations in the $|LSL_zS_z\rangle$ space are more physically appropriate due to their completeness, but traditional calculations with base $|JJ_z\rangle$ can be also performed by our computation systems for comparisons and rapid estimations [2]. For calculating properties in temperatures around the magnetic phase transition point, a self-consistent methodology for molecular field calculation called Mean Field Approximations (MFA) is applied. The idea behind this method is to estimate the direction and value of the magnetic field (molecular field) generated by ions at a defined temperature, and to calculate the influence of this magnetic field for electronic state structures of ions. In a selected calculation space, according to eq.1 we define a molecular field as an expected value of the total moment of the 4f electronic subshell multiplied

by the molecular field, inter ionic exchange factor n_{mol}:

$$\mathbf{B}_{mol} = -n_{mol}\, g_L \mu_B < \mathbf{J} > \quad (4)$$

or

$$\mathbf{B}_{mol} = -n_{mol}\, \mu_B < \mathbf{L} + g_e \mathbf{S} > \quad (5)$$

Where the gyromagnetic factors are g_L and $g_e \approx 2.002319$. On the basis of the calculated electronic level structure $E_i(T)$, the directional components of magnetic moments are established for all identical ions. This means that Hamiltonian matrix diagonalization is performed for all defined temperature steps recurrently. This is in contrast to simple ATOMIC MATTERS calculations [1], which diagonalize matrices one time for a single run and deduce all thermodynamic properties from the stable discrete energy level structure obtained. This self-consistent procedure provides temperature-dependent energy level structure and has one only free parameter, n_{mol}, called the molecular field parameter. The value of n_{mol} is closely related to the phase transition temperature T_C of the macroscopic structure of ions. The formal expression of the full Hamiltonian used by ATOMIC MATTERS MFA computation system, according to the chosen calculation space: $|JJ_z>$ or $|LSL_zS_z>$ respectively, has the form:

$$H_{J\,mol} = H_J + H_{mol} = +\sum_n \sum_m B_n^m \hat{\mathbf{O}}_n^m(J, J_z) + + n_{mol}\, g_L^2\, \mu_B^2 \left(-\mathbf{J} < \mathbf{J} > + \frac{1}{2} < \mathbf{J} >^2 \right) + g_L\, \mu_B\, \mathbf{J} \cdot \mathbf{B}_{ext} \quad (6)$$

or

$$H_{LS\,mol} = \sum_n \sum_m B_n^m \hat{\mathbf{O}}_n^m(L, L_z) + \lambda \mathbf{L} \cdot \mathbf{S} + + n_{mol}\, \mu_B^2 \left(-(\mathbf{L} + g_e \mathbf{S}) < \mathbf{L} + g_e \mathbf{S} > + \frac{1}{2} < \mathbf{L} + g_e \mathbf{S} >^2 \right) + + \mu_B (\mathbf{L} + g_e \mathbf{S}) \cdot \mathbf{B}_{ext} \quad (7)$$

The eigenvectors of the Hamiltonian are described, according to the selected calculation base, by the total momentum quantum numbers $|JJ_z>$ or spin and orbit quantum numbers $|LSL_zS_z>$. Using the commutation relations of the angular momentum operators, we obtain information about expected values of the projections of magnetic momentum of all electronic states at a chosen temperature [2]:

$$m_J^{\alpha}(T) = \frac{g_L \mu_B}{Z(T)} \sum_i < J_\alpha^i > \exp\left(-\frac{E_i(T)}{k_B T} \right) \quad (8)$$

$$m_{LS}^{\alpha}(T) = \frac{\mu_B}{Z(T)} \sum_i < L_\alpha^i + g_e S_\alpha^i > \exp\left(-\frac{E_i(T)}{k_B T} \right) \quad (9)$$

Where: α indexes directional components, i numbers the Hamiltonian eigenstates, while Γ_i represents the expected value of the total angular momentum along the α-axis in the i-th state:

$$<J_\alpha^i> = <\Gamma_i(T)|\, \mathbf{J}_\alpha \,|\, \Gamma_i(T)> \quad (10)$$

$$<L_\alpha^i + g_e S_\alpha^i> = <\Gamma_i(T)|\, \mathbf{L}_\alpha^i + g_e \mathbf{S}_\alpha^i \,|\, \Gamma_i(T)> \quad (11)$$

All property calculations can be done for 3D (x,y,z) real space by using complex Hamiltonian matrix elements defined by full expressions of extended Stevens $\mathbf{O}^m_n$ operators[10]. Mostly for comparison with traditional calculation results, ATOMIC MATTERS also offers a 2D (x,z) calculation methodology of a simplified model of CEF interactions defined by Stevens $\mathbf{O}^m_n$ operators with real number matrix elements only [12].

Taking into consideration the possibility of the thermal population of states, we automatically obtain the thermal evolution of single ion properties of the whole compound [11,12].

Under the thermodynamic principle at temperature T=0K, only the ground state is occupied. In this situation, the magnetic moment of the ion is exactly equal to the momentum of the ground state. If the temperature rises, the probability of occupying higher states increases according to Boltzmann statistics. The number of ions with energy E_i within a system at temperature T is:

$$N_i(T) = N_0 \frac{\exp\left(-\frac{E_i(T)}{k_B T} \right)}{Z(T)} \quad (12)$$

where $N_0 \approx 6.022.1023\ mol^{-1}$ (Avogadro constant) and $Z(T)$ is the sum of states. Knowing the sum of the states, we can determine the Helmholtz free energy $F(T)$:

$$F(T) = -k_B T \ln Z(T) \quad (13)$$

According to thermodynamic principles, the contribution of localized electrons to the total specific heat of materials can be calculated by numerical derivation of Helmholtz free energy:

$$c_{mol}(T) = -T \left(\frac{\partial^2 F(T)}{\partial T^2} \right) \quad (14)$$

This makes it possible to calculate entropy according to the well-known definition:

$$S(T) = S(0) + \int_0^T \frac{c(T)}{T} dT \quad (15)$$

The value of electronic entropy for a defined temperature is difficult to compare, but the isothermal change of the entropy of the system at a given temperature is a very important material parameter that describes its thermomagnetic properties. Isothermal Entropy change $-\Delta S(T, B_{ext})$, captured for different temperatures under the

influence of different magnetic fields, is one the most important properties of a material that describes its usefulness as a magnetocaloric material. The value $\Delta S(T, B_{ext})$, extracted from experimental specific heat measurements, is often presented as a basic description of the Magnetocaloric Effect (MCE) of a material [3-7]. In our approach, isothermal entropy change can be directly calculated from eq. 15 according to the definition:

$$\Delta S(T, \mathbf{B}_{ext}), = S(T, \mathbf{B}_{ext}=0)-S(T, \mathbf{B}_{ext}). \quad (16)$$

ATOMIC MATTERS MFA also provides single-ionic magnetocrystalline anisotropy calculations that include full calculations (without Brillouin function approximation) of $K_i(T)$ magnetocrystalline constants for defined temperature ranges according to the relations [15]:

$$K_1(T) = \frac{3}{2}B_2^0\left(\left\langle \hat{\mathbf{O}}_2^0\right\rangle - \left\langle \hat{\mathbf{O}}_2^2\right\rangle\right) - 5B_4^0\left(\left\langle \hat{\mathbf{O}}_4^0\right\rangle - 3\left\langle \hat{\mathbf{O}}_4^2\right\rangle\right) - \\ - \frac{21}{2}B_6^0\left(\left\langle \hat{\mathbf{O}}_6^0\right\rangle - 5\left\langle \hat{\mathbf{O}}_6^2\right\rangle\right),$$

$$K_2(T) = \frac{35}{8}B_4^0\left(\left\langle \hat{\mathbf{O}}_4^0\right\rangle - 4\left\langle \hat{\mathbf{O}}_4^2\right\rangle + \left\langle \hat{\mathbf{O}}_4^4\right\rangle\right) + \\ + \frac{63}{8}B_6^0\left(\left\langle \hat{\mathbf{O}}_6^0\right\rangle - 20\left\langle \hat{\mathbf{O}}_6^2\right\rangle + 5\left\langle \hat{\mathbf{O}}_6^4\right\rangle\right),$$

$$K_2^*(T) = \frac{1}{8}\left(B_4^0\left\langle \hat{\mathbf{O}}_4^0\right\rangle + 5B_6^4\left\langle \hat{\mathbf{O}}_6^4\right\rangle\right),$$

$$K_3(T) = -\frac{231}{16}B_6^0\left\langle \hat{\mathbf{O}}_6^0\right\rangle,\ K_3^*(T) = -\frac{11}{16}B_6^4\left\langle \hat{\mathbf{O}}_6^4\right\rangle. \quad (17)$$

Where: $\left\langle \hat{\mathbf{O}}_n^m\right\rangle$ denotes thermal expected values of Stevens operators we defined according to C. Rudowicz [10]. The exchange interactions simulated according to MFA methodology defined by eq. 1 provides simulated properties strongly dependent on the only parameter n_{mol} that is closely related to the temperature of phase transitions: T_C. It is easy to find the value of n_{mol} for correct T_C, but the value of this parameter can be estimated according to De Gennes scaling [11]:

$$T_C \sim G(f^n),\ G(f^n)=(g_L-1)^2J(J+1) \quad (18)$$

De Gennes scaling is also a useful tool for n_{mol} estimation, as charge surroundings can be transferred between ions in series. The CEF part of Hamiltonian contains Stevens CEF parameters B^m_n. The values of these parameters are only appropriate for the defined ion. The recalculation of B^m_n parameters defined for an ion A in the crystal lattice surrounding of ion B in the same crystalline position follows the simple scheme:

$$B^m_n \text{ (ion A)} \rightarrow A^m_n \rightarrow B^m_n \text{ (ion B)} \quad (19)$$

Stevens B^m_n parameters can be expressed by universal A^m_n parameters, according to the calculation space used, as follows:

$$|J,J_z\rangle;\ B^m_n(J,J_z)=\theta_n(J)\langle r_{4f}{}^n\rangle A^m_n$$
$$|L,S,S_z,L_z\rangle;\ B^m_n(L,L_z)=\theta_n(L)\langle r_{4f}{}^n\rangle A^m_n \quad (20)$$

Where values of the 2nd, 4th and 6th power of average radius of a/the 4f shell $\langle r^n\rangle$ have been calculated by many authors using Hartree-Fock-type methodology, and the results can be easily found in the literature. The θ_n parameters are the J or L dependent Clebsh-Gordan-type factors, sometimes called $\alpha.\beta,\gamma$ Stevens factors $\theta_2=\alpha$, $\theta_4=\beta$, $\theta_6=\gamma$, which can be expressed by finite equations available in [12-14]. The values of $\langle r_{4f}{}^n\rangle$ are collected in the system's open database together with a reference. In all presented calculations for R ions, we used the $\langle r_{4f}{}^n\rangle$ values tabulated in [14]. The ability to recalculate CEF parameters between ions and calculation spaces offers a unique chance to establish an acceptable simplification of methodology. The recalculation of CEF parameters in Atomic Matters systems is fully automated, but an explicit Stevens Factors Calculator is also available.

4 Calculation results

In this section, we present the results of an investigation of the magnetic and magnetocaloric properties of a $HoAl_2$ and $ErAl_2$ single crystal. The predictions of properties are completely achieved without free parameters. We use established cubic CEF for $DyAl_2$ [parallel paper] parameters in Stevens notation [3] $B_4=-(5.5\pm1.2)\cdot10^{-5}$ meV and $B_6=-(5.6\pm0.8)\cdot10^{-7}$ meV. We recalculated values of Stevens parameters to universal, ion-independent CEF notation A^m_n according to eq. 19 and eq. 20. We assume that the parameters $A_4=+7.164Ka_0$ and $A_6=-1.038Ka_0$ that are obtained in this way define the charge surroundings of an R ion in a crystal lattice of RAl_2. The visualization of such defined potential is shown in fig. 2. The triangular shapes, which related with the location of the coordinating Al ions, are located symmetrically in cubic surroundings and reflect the atom position visible in the elementary cell of Laves phase shown in fig. 2.

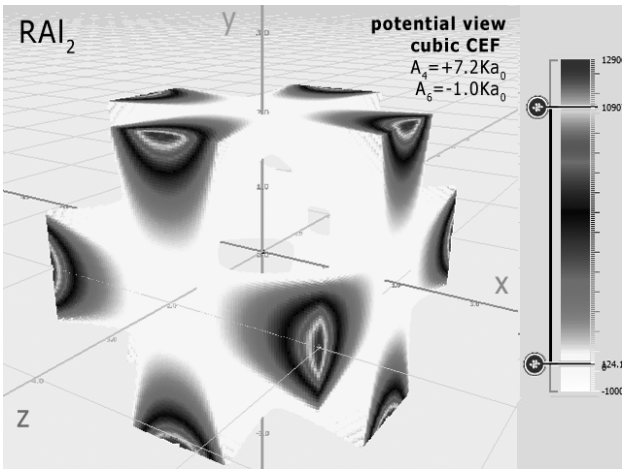

Fig.2. Crystal Field potential visualization of cubic surrounding of R-ions in RAl_2, defined by CEF parameters: A_4=+7.164Ka_0 and A_6 =-1.038Ka_0. The visualization of positive sign potential is externally cut off by the cube.

We attributed the magnetism of $HoAl_2$ and $ErAl_2$ and the magnetism of $HoAl_2$ to the Ho ions and performed calculations of the fine electronic structure of the $4f^{10}$ and $4f^{11}$ electronic systems, respectively. All calculations was performed for cubic symmetry, taking into account the crystal field and inter-site, spin-dependent exchange interactions. The energy level scheme derived is associated with the reduction of the degeneracy of the lowest atomic term (^{5}**I** and ^{4}**I** for Ho and Er ions, respectively) given by Hund's first two rules. The value of molecular field factor n_{mol} for $HoAl_2$ and $ErAl_2$ was established according to $n_{mol}^{Dy} = 3.6T/\mu_B$ for $DyAl_2$ and de Gennes scaling eq. 18 [11]. The comparison between experimentally found Curie temperature T_C and de Gennes scaling is shown in fig.3

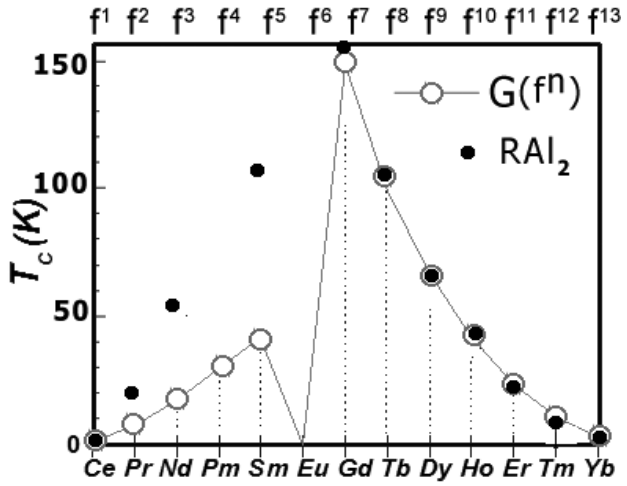

Fig.3. De Gennes scaling of Curie temperature T_C for all rare-earth ions in series RAl_2 in comparison to experimental data from ref.[3].

Experimental values of T_C for RAl_2 compounds [3-7] and the theory are in good agreement for 'heavy Rare Earths'elements from Gd ($4f^7$) to Yb($4f^{13}$). De Genes relations [10,14] makes it possible to establish molecular field factor for $HoAl_2$ n_{mol}^{Ho}=2.1T/μ_B and for $ErAl_2$ n_{mol}^{Er}=0.95T/μ_B.

4.1 Calculated properties of $HoAl_2$ single crystals.

The electronic configuration of $_{67}$Ho atoms consists of a closed shell inactive atomic core [$_{54}$Xe], electronic system $4f^{10}$ and 'outer electrons $5d^16s^2$. We attributed the magnetic properties of $HoAl_2$ compound as an effect of properties of $4f^{10}$ electronic system under influence of electromagnetic interactions defined according to the description in the theory section. The starting point of our analysis is the ground atomic term ^{5}I with quantum number of orbital angular momentum L=6 and total spin S=2.

The full calculated energy level structure in |L,S,Lz,Sz> calculation space is shown in fig. 4. The obtained overall splitting is strongly dependent on the strength of spin–orbit intra-atomic interactions. We used free-ion value of spin orbit constant of Ho^{3+} ions λ=-780K [13] and obtained overall splitting of ^{2}F atomic term at about 20350K = 1.753 eV.

Details of ground states structure are shown in fig. 4.

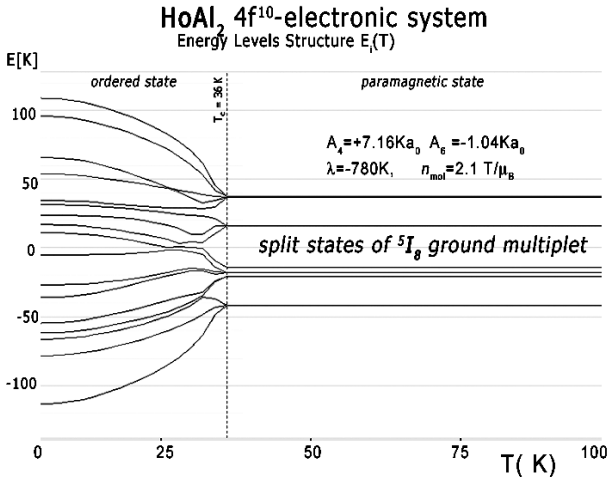

Fig.4. The result of calculation of ground multiplet energy levels structure vs. temperature calculated vs. temperature of the fine electronic structure of $4f^{10}$ electronic configuration of Ho ions in $HoAl_2$ in

|L,S,Lz,Sz>. At Curie temperature T_C =36K structure splits under the influence of molecular field.

In the absence of an external magnetic field, the induced molecular field splits and moves into degenerated states. The value of the molecular field factor established for $HoAl_2$ which reproduce T_C well at about 36K is n_{mol}=2.1T/μ_B.

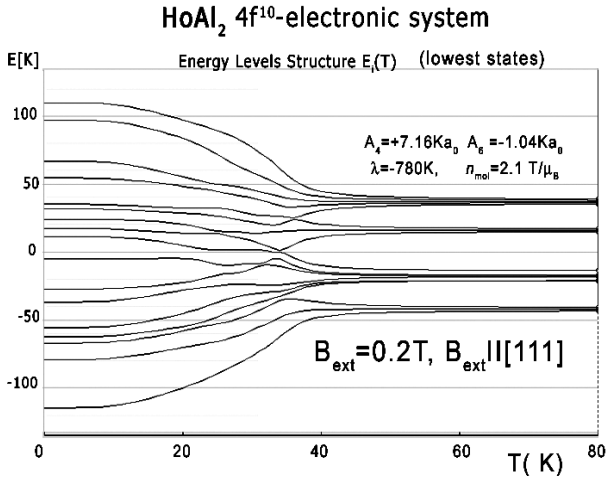

Fig. 5. Ground multiplet energy levels structure vs. temperature calculated for $4f^{10}$ electronic system of Ho ions in $HoAl_2$ under the influence of a small external magnetic field of 0.2T applied along crystal direction [111].

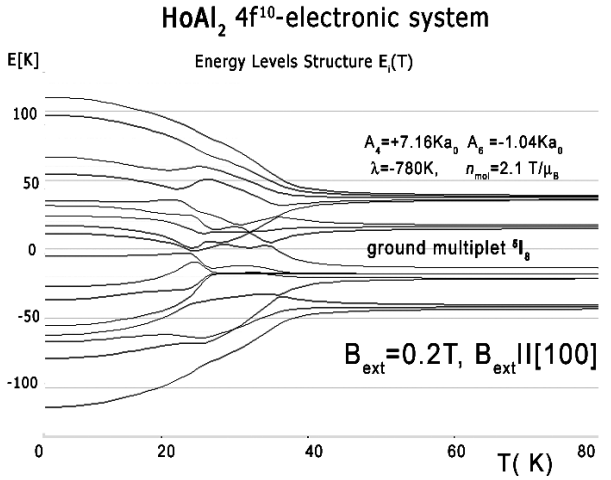

Fig. 6. Ground multiplet energy levels structure vs. temperature calculated for $4f^{10}$ electronic system of Ho ions in $HoAl_2$ under the influence of a small external magnetic field of 0.2T applied along crystal direction [111].

Above T_C, in a paramagnetic state, the ground state is degenerated and consist of 3 states. The ground triplet wave functions of ground state of Ho ions ($4f^{10}$ electronic system) in $HoAl_2$ in a paramagnetic state can be expressed in |Jz> notation as:

Γ_1= +0.4|-6> +0.583|-2> -0.583|+2> -0.4|+6>

Γ_2 = -0.086|-5>-0.367|-1>+0.5807|+3> +0.72|+7>
Γ_3 = -0.086|+5>-0.367|+1>+0.581|-3> +0.722|-7>

A molecular field split these states at $T<T_C$. The value of the molecular field changes, and at T=0 (absolute zero) B_{mol}=13T and its direction is along crystal direction [110]. In this condition, the wave function of a ground singlet gets the form:

Γ_0= -0.291|-8>+0.588|-7> -0.410|-6> +0.223|-5> -0.257|-4> +0.38|-3> -0.312|-2> +0.151|-1> -0.014|0> -0.081|+1> +0.09|+2> -0.040|+3> +0.010|+4> -0.011|+5> +0.018|+6> -0.012|+7> +0.002|+8>

The electronic structure obtained in the absence of an external magnetic field is fragile; even a small magnetic field applied along direction [100] or [111] forces the structure to change the order of states and creates an anomaly at low temperatures. The influence of a small external magnetic field applied along direction [111] for the structure of the lowest electronic states is shown in fig. 6. The position of this anomaly corresponds with peaks on specific heat curves. The calculated specific heat for a $HoAl_2$ single crystal under the influence of an external magnetic field applied along various crystal directions is presented in fig. 7, fig. 8 and fig. 9.

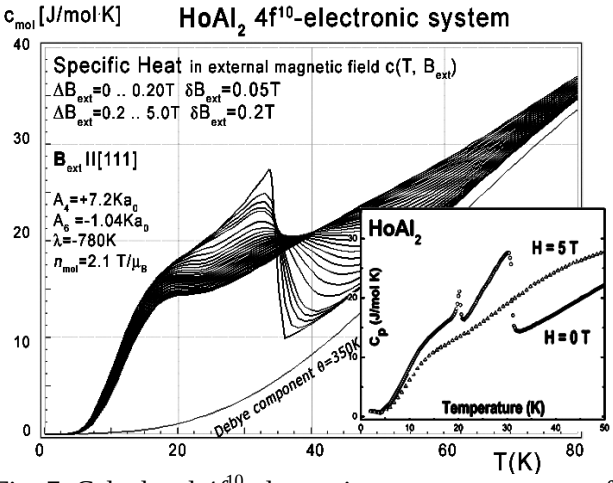

Fig. 7. Calculated $4f^{10}$-electronic system component of molar specific heat (eq.14) with Debye crystal lattice component (θ=350K) vs. temperature for Ho ions in $HoAl_2$, under the influence of an external magnetic field applied along direction [100]. Inset: experimental data from ref.[4].

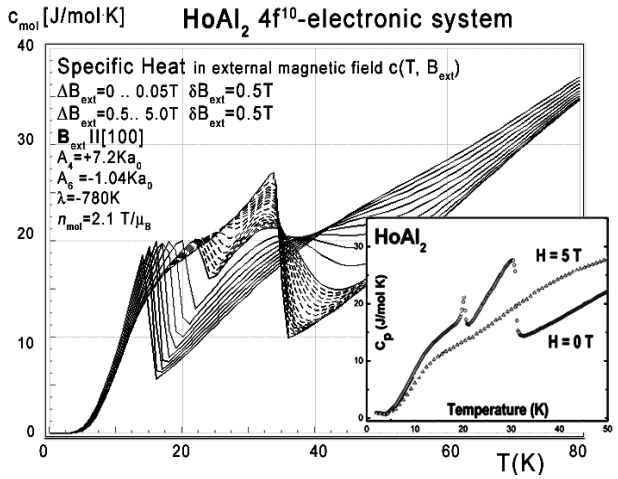

Fig. 8. Calculated molar specific heat (eq.14) vs. temperature for Ho ions in $HoAl_2$, under the influence of an external magnetic field applied along [100] direction. Inset: experimental data from ref.[4].

The closer look at the unusual behaviour of the 4*f*- electron component of specific heat simulated under the influence of an external magnetic field along 'diagonal' direction [111] is shown in fig.10.

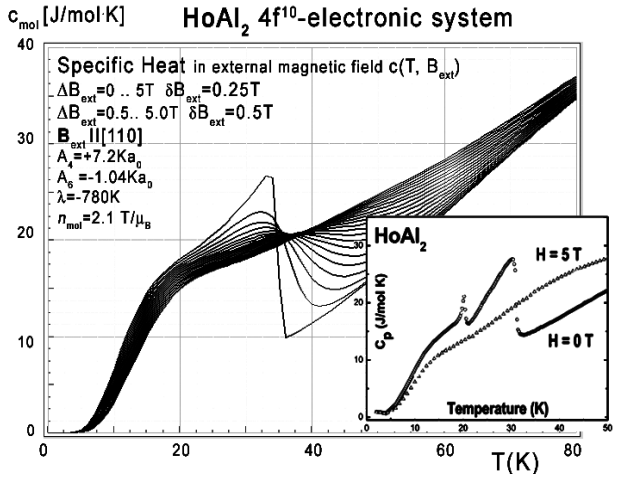

Fig. 9. Calculated molar specific heat (eq.14) vs. temperature for Ho ions in $HoAl_2$, under the influence of an external magnetic field applied along easy magnetization axis, direction [100]. Inset: experimental data from ref.[4].

We have not found comparative experimental data for specific heat measurements, but F. W. Wang [5] provides data of measured specific heat change $\Delta c(T,B_{ext})$ defined as:

$$\Delta c(T,B_{ext}) = c(T,B_{ext}) - c(T,0) \qquad (21)$$

for measurements for ΔB_{ext}=5T. Comparison between data from [5] and our simulations of $\Delta c(T,B_{ext})$ is shown in fig.11. The simulation for ΔB_{ext}=5T in this figure is represented by a solid line.

Collected data of specific heat makes it possible to calculate isothermal entropy change $-\Delta S(T, B_{ext})$ according to eq.16, the same methodology as used by experimentalist [3-7]. Isothermal entropy changes calculated with various external magnetic fields applied along all main directions of the/a cubic structure are presented in fig. 10, fig.11 and fig.12.

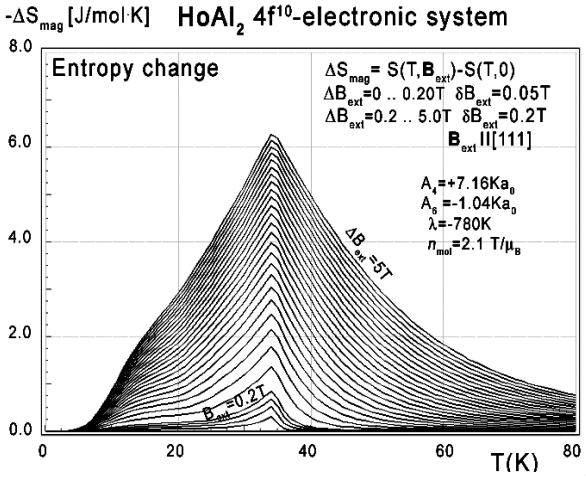

Fig. 10. Calculated isothermal entropy change of $4f^{10}$-electronic system vs. temperature (eq.16) of Ho ions in $HoAl_2$, under the influence of various external magnetic field values from 0 to 0.2T, with step 0.05T and from 0 to 0.2 to 5.0T, with step 0.2T applied along direction [111].

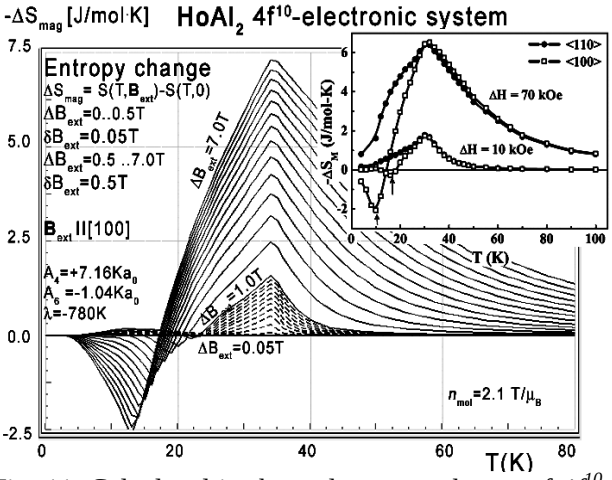

Fig. 11. Calculated isothermal entropy change of $4f^{10}$-electronic system vs. temperature (eq.16) of Ho ions in $HoAl_2$, under the influence of various external

magnetic field values from 0 to 0.5T, with step 0.05T and from 0 to 0.5 to 7.0T, with step 0.5T applied along direction [100]. Inset: experimental data from ref.[5].

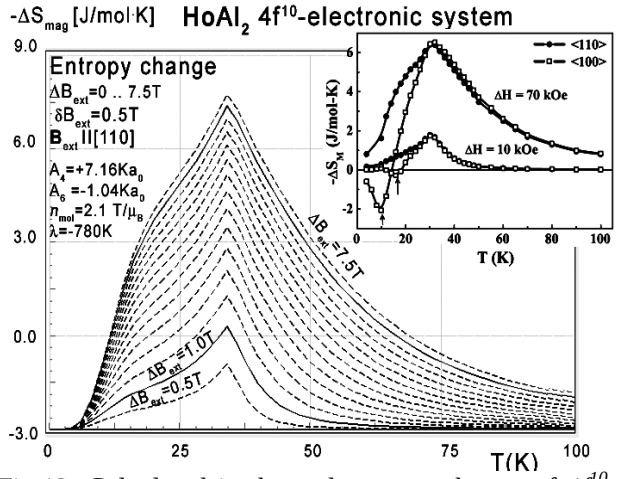

Fig.12. Calculated isothermal entropy change of $4f^{10}$-electronic system vs. temperature (eq.16) of Ho ions in $HoAl_2$, under the influence of various external magnetic field values from 0 to 7.5T, with step 0.5T applied along direction [111]. Inset: experimental data from ref.[5].

The anisotropic behavior of calculated thermomagnetic properties is reflected in magnetocrystalline anisotropy constant calculations. The results of $K_i(T)$ calculations according to eq.17 in the absence of an external magnetic field are shown in fig. 14.

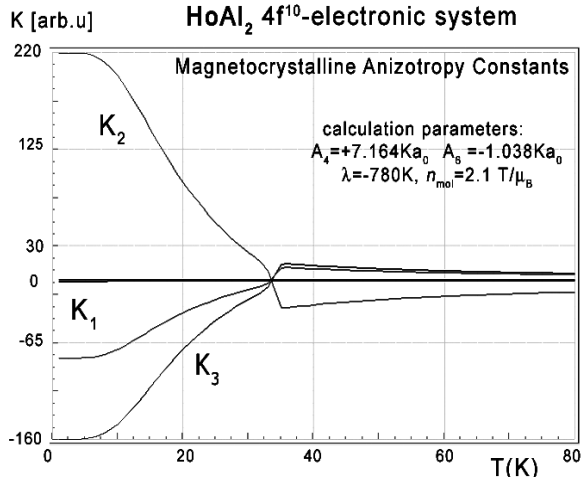

Fig.13. Calculated according eq.17 magnetocrystalline anisotropy constants K_1,K_2 and K_3 vs. temperature, calculated for Ho ions in $HoAl_2$ in absence of external magnetic field.

The results of $K_i(T)$ calculations according to eq.17 under the influence of external magnetic field B_{ext}=1T applied along direction [100] are shown in fig. 14.

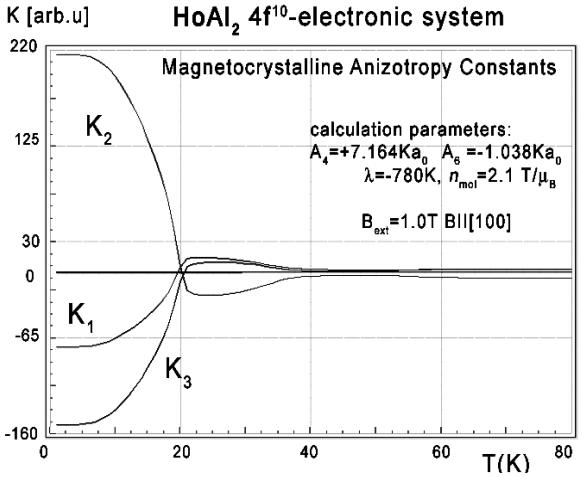

Fig. 14. Calculated according eq.17 magnetocrystalline anisotropy constants K_1,K_2 and K_3 vs. temperature, calculated for Ho ions in $HoAl_2$ under influence of CEF and molecular magnetic field.

For completeness, magnetic moment calculations vs. temperature under various external magnetic field conditions were performed. The results of $\mathbf{m}(T,\mathbf{B}_{ext})$ are presented in fig. 15, fig. 16 and fig.17. The simulated thermal evolution of magnetic moment components under the influence of external magnetic field along direction [110] shown in fig. 16 clearly confirms direction [110] as an easy magnetization axis of $HoAl_2$ in the lowest temperatures The applied external magnetic field along this direction confirms perfect parallel directions of magnetic vector and induced external magnetic field.

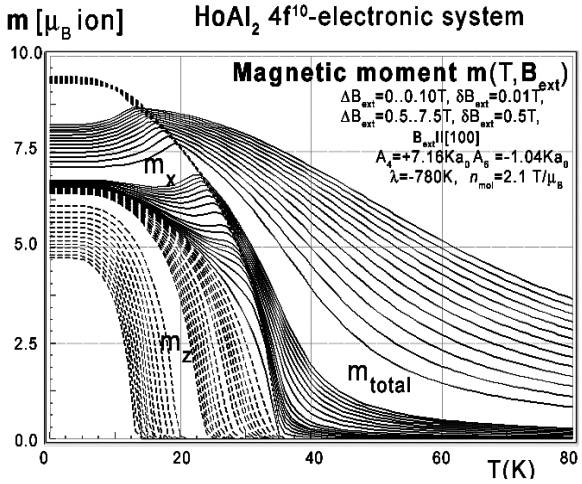

Fig. 15. Calculated x,y,z-directional components of total magnetic moment vs. temperature, calculated for Ho ions in $HoAl_2$ the influence of various external magnetic field values from 0 to 0.1T, with step 0.01T

and from 0.5 to 7.5T with step 0.5T applied along direction [100].

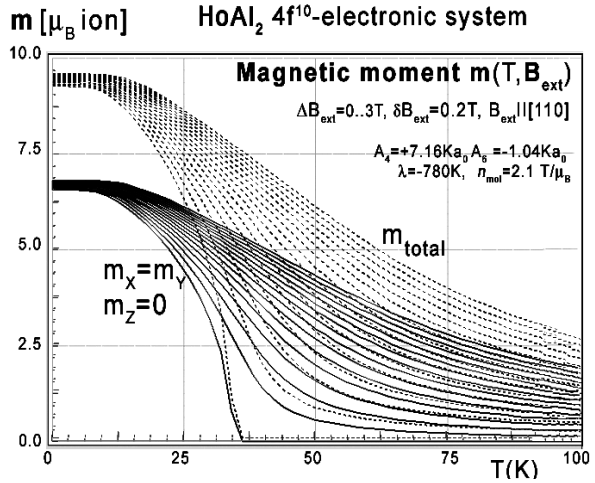

Fig.16. Calculated x - components (solid lines), z-components (dashed lines) of total magnetic moment m_{total} (doted lines) vs. temperature, calculated for Ho ions in $HoAl_2$ under influence of CEF, molecular magnetic field and various values of external magnetic field from 0 to 3T with step 0.2T applied along direction [110].

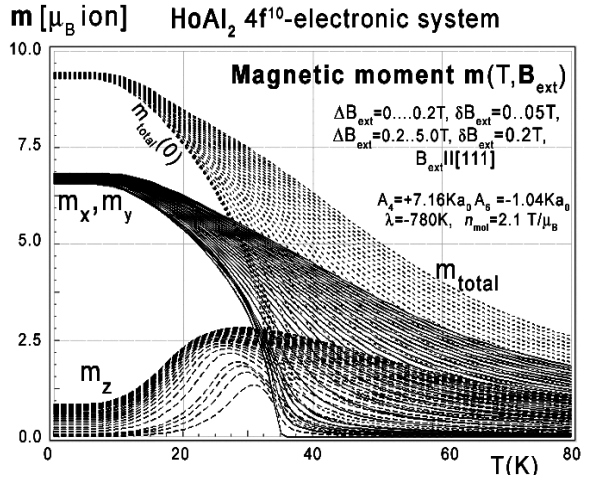

Fig. 17. Calculated x,y,z-directional components of total magnetic moment vs. temperature, calculated for Ho ions in $HoAl_2$ under influence of CEF and molecular magnetic field and various values of external magnetic field from 0 to 0.2T, with step 0.05T and from 0.2 to 5.0T with step 0.2T applied along direction [111].

.

Magnetic moment calculated in external magnetic field parallel to [111] and [100] direction reveals unusual behavior of the directional component of total moment. Similar behavior of magnetic moment directions was reported in ref. [4], but most of the presented results of calculations of properties of $HoAl_2$ still await experimental verification.

We found only a few reports about measurements of thermomagnetic properties of $HoAl_2$ single crystals. Some experimental comparative data of isothermal entropy change measured on $HoAl_2$ single crystals is provided by L.A. Gil et al. [4], and interesting entropy change is provided by M. Patra at al. [5]. All experimental data from [4,5] confirms the correctness of our approach in thermomagnetic properties calculations of of $HoAl_2$.

4.2 Calculation results for $ErAl_2$ single crystals.

The electronic configuration of Er atoms consists of a closed shell inactive atomic core [$_{54}$Xe], electronic system $4f^{11}$ and 'outer electrons' $5d^16s^2$. We attribute the magnetic properties of $ErAl_2$ compound to be an effect of properties of $4f^{11}$ electronic system under the influence of electromagnetic interactions defined according to the description in the theory section. The starting point of our analysis is the ground atomic term ^{4}I with quantum number of orbital angular momentum L=6 and total spin S=3/2.

The full calculated energy level structure in |L,S,Lz,Sz> calculation space reveals good separation of ground multiplet $^4I_{15/2}$ states from the rest of eigenstates of the fine electronic structure. The overall energy levels splitting is strongly dependent on the strength of spin–orbit intra-atomic interactions. We used free-ion value of spin orbit constant of Er^{3+} ions λ=-1170K [13] and obtained overall splitting of ^{4}I atomic term at about 22900K=1.97 eV. Details of ground multiplet $^4I_{15/2}$ states structure are shown in fig.18.

In the absence of an external magnetic field, the induced molecular field at $T<T_C$ splits degenerated states. The value of the molecular field factor established according to de Gennes scaling [10] for $ErAl_2$ which reproduce T_C well at about 11K is n_{mol}=0.95T/μ_B. Above T_C, in a paramagnetic state, the ground state is degenerated. The ground quartet consists of two quasi doublets. The wave functions of ground state of Er ($4f^{11}$ electronic system) ions in $ErAl_2$ in a paramagnetic state can be expressed in |Jz> notation as:

Γ_1=-0.44|-6.5>+0.72|-2.5>+0.458|+1.5>-0.29|+5.5>

Γ_1^*=-0.44|+6.5>+0.72|+2.5>+0.458|-1.5>-0.28|-5.5>

Γ_2=-0.61|-7.5>+0.78|-3.5>+0.143|+0.5>-0.04|+4.5>

Γ_2^*=0.61|+7.5>0.781|+3.5>+0.14|-0.5>+-0.04|-4.5>

A molecular field split these states at $T<T_C$. The value of the molecular field changes, and at T=0 (absolute zero) B_{mol}=4.46T and its direction is along

crystal direction [110]. In this condition, the wave function of a ground singlet gets the form:

Γ_0=-0.483|-7.5>+0.32|-6.5>-0.111|-5.5>-0.12|-4.5>+ +0.577|-3.5>-0.459|-2.5>+0.159|-1.5>-0.029|-0.5>+ +0.104|+0.5>-0.185|+1.5>+0.116|+2.5>-0.03|+3.5>- -0.017|+4.5>+0.066|+5.5>-0.048|+6.5>+0.015|+7.5>

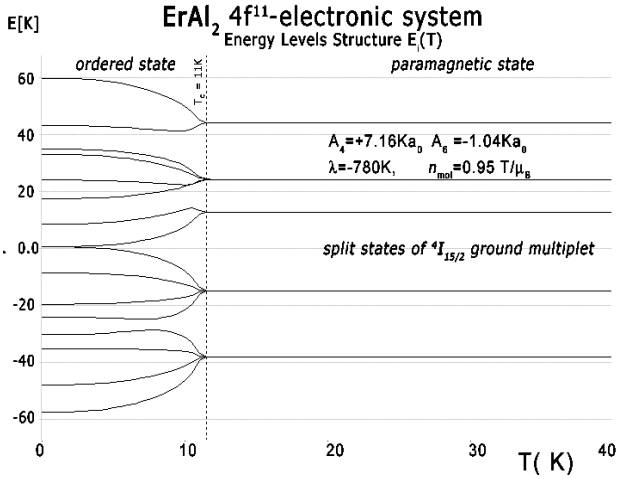

Fig. 18. The result of calculation of energy level positions vs. temperature of the fine electronic structure of $4f^{11}$ electronic configuration of Er ions in $ErAl_2$

The structure of states is sensitive on external magnetic field influence. The effect of an external magnetic field B_{ext}=1T applied along direction [111] for the structure of the lowest electronic states is shown in fig. 19.

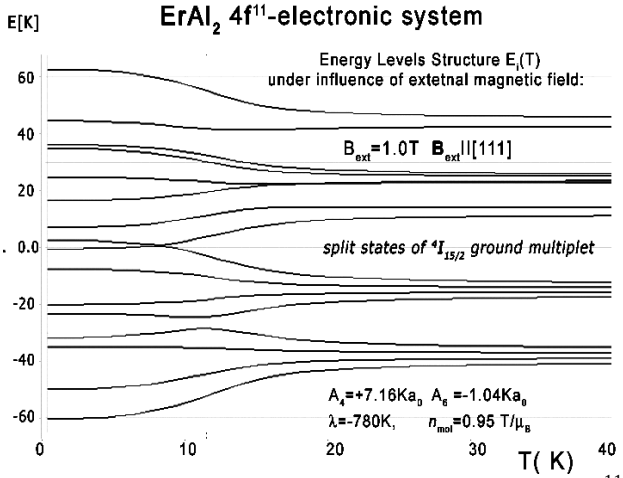

Fig. 19. Calculated energy level structure of $4f^{11}$ electronic system of Er ions vs. temperature under the influence of external magnetic field B_{ext}=1T applied along direction[111].

The energy level structure makes it possible to calculate the 4*f*-electron component of specific heat.

The result of calculation of specific heat under the influence of an external magnetic field compared to experimental data from ref. [8] is shown in fig. 20, fig. 21 and fig. 22.

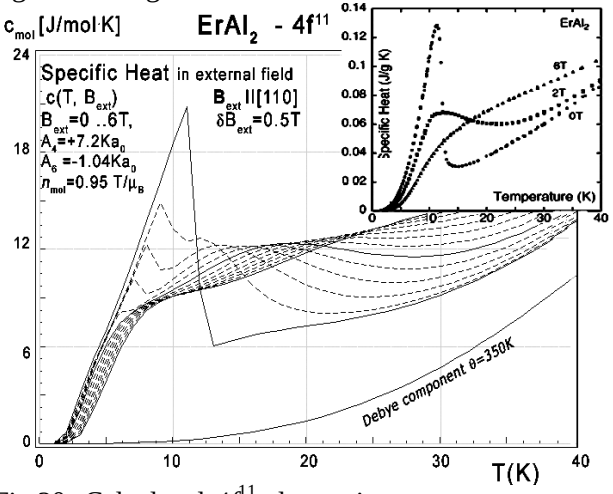

Fig.20. Calculated $4f^{11}$-electronic system component of molar specific heat (eq.14) with Debye crystal lattice component (θ=350K) vs. temperature of Er ions in $ErAl_2$, under the influence of external magnetic field from 0 to 6T with step 0.2T. Inset: experimental data from ref. [8] Congruent with experimental, calculated for B_{ext}=0 B_{ext}=2.0T and B_{ext}=6.0T lines are solid lines.

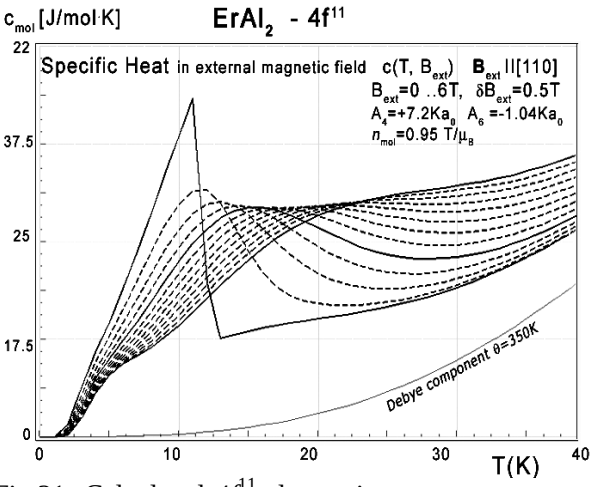

Fig.21. Calculated $4f^{11}$-electronic system component of molar specific heat (eq.14) with Debye crystal lattice component (θ=350K) vs. temperature of Er ions in $ErAl_2$, under the influence of external magnetic field from 0 to 6T with step 0.2T.

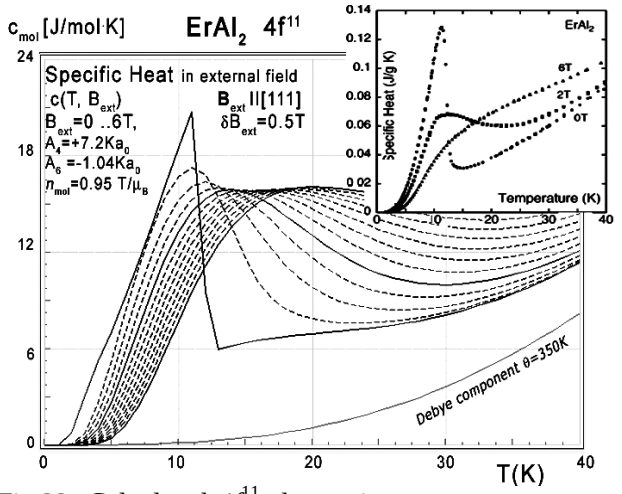

Fig.22. Calculated $4f^{11}$-electronic system component of molar specific heat (eq.14) with Debye crystal lattice component (θ=350K) vs. temperature of Er ions in $ErAl_2$, under the influence of external magnetic field from 0 to 6T with step 0.2T. Inset: experimental data from ref. [8] Congruent with experimental, calculated for B_{ext}=0 B_{ext}=2.0T and B_{ext}=6.0T lines are solid lines.

Collected specific heat data makes it possible to calculate isothermal entropy change $-\Delta S(T, B_{ext})$ according to eq.16, the same methodology as used by experimentalist [3-8]. Isothermal entropy change calculated with various external magnetic fields is presented in fig. 23, fig. 24 and fig. 25.

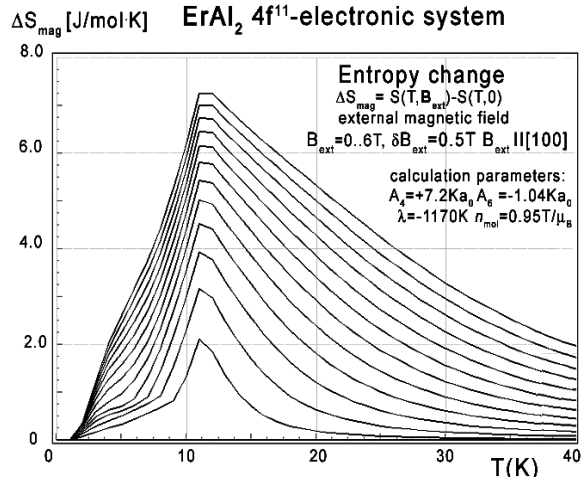

Fig.23. Calculated isothermal entropy change of $4f^{11}$-electronic system vs. temperature (eq.16) of Er ions in $ErAl_2$, under influence of various values of external magnetic field from 0 to 6T, with step 0.2T applied along [100] direction.

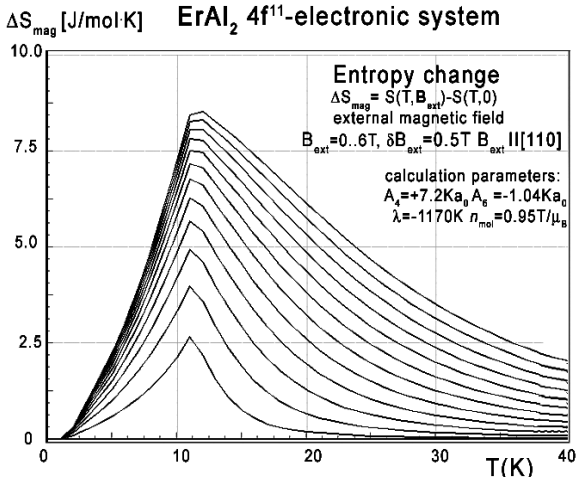

Fig.24. Calculated isothermal entropy change vs. temperature (eq.16) for various values of external magnetic field from 0 to 6.0T with step 0.5T, applied along [110] direction of $ErAl_2$ crystal lattice.

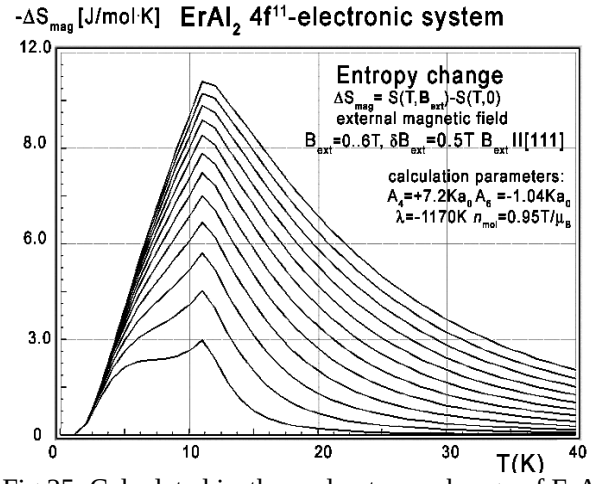

Fig.25. Calculated isothermal entropy change of $ErAl_2$ vs. temperature (eq.16) for various values of external magnetic field from 0 to 6T with step 0.5T, applied along diagonal [111] direction.

The anisotropic behavior of calculated thermomagnetic properties reflects in magnetocrystalline anisotropy constant calculations. The results of $K_i(T)$ calculations according to eq.17 in absence of external magnetic field are shown on fig.12.

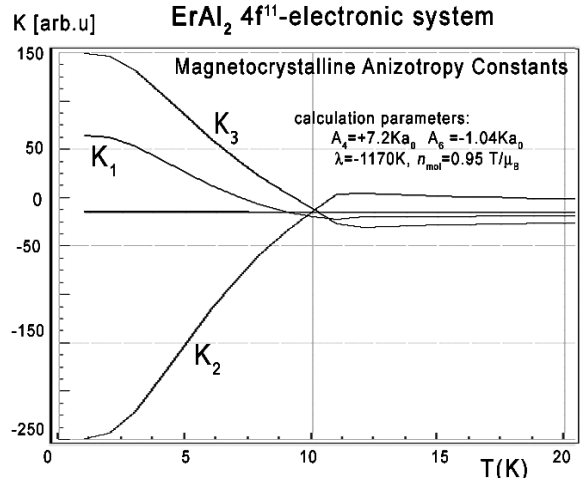

Fig.26. Calculated according eq.17 magnetocrystalline anisotropy constants K_1,K_2 and K_3 vs. temperature, calculated for Er ions under influence of CEF established for RAl_2 series and molecular magnetic field.

For completeness, magnetic moment calculations vs. temperature under various external magnetic field conditions was performed. The results of $\mathbf{m}(T,\mathbf{B}_{ext})$ are presented in fig. 27, fig. 28 and fig. 29.

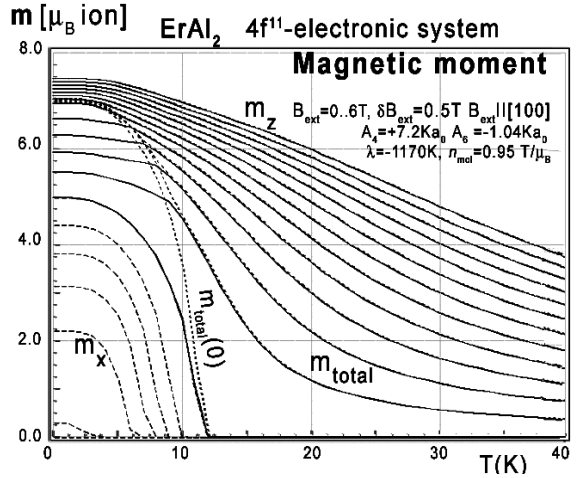

Fig.27. Calculated x,y,z-directional components of total magnetic moment vs. temperature, calculated for Er ions in $ErAl_2$ under influence of CEF and molecular magnetic field and various values of external magnetic field from 0 to 6T with step 0.5T applied along direction [100].

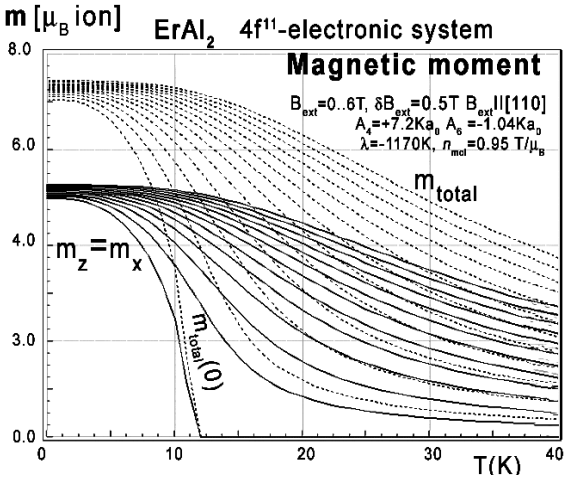

Fig.28. Calculated x,y,z - components of total magnetic moment m_{total} (doted lines) vs. temperature, calculated for Er ions in $ErAl_2$ under influence of CEF, molecular magnetic field and various values of external magnetic field from 0 to 6T with step 0.5T applied along direction [110]. $m_y(T)=0$, x and z – components of magnetic moment are equally distributed.

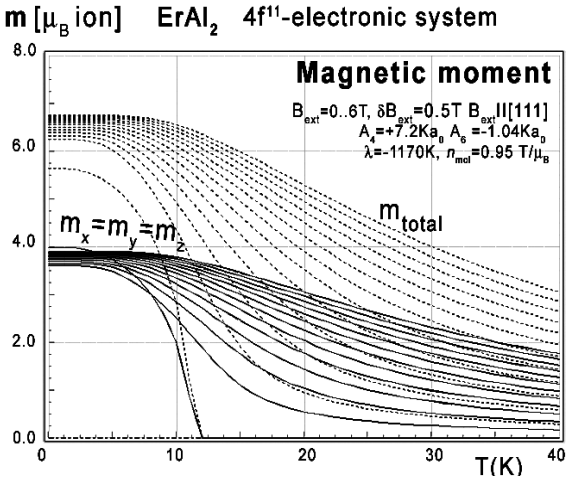

Fig.29. Calculated x,y,z - components of total magnetic moment m_{total} (doted lines) vs. temperature, calculated for Er ions in $ErAl_2$ under influence of CEF, molecular magnetic field and various values of external magnetic field from 0 to 6T with step 0.5T applied along direction [111]. All directional magnetic moment components are equally distributed.

Magnetic moment calculated in external magnetic field parallel to [111] and [110] direction reveals unusual behavior of the directional component of total moment. The electronic system seems to be easy switchable between those crystallographic directions. The low temperature easy magnetization axis along direction [110] easy transforms into [111]. The external magnetic field under B_{ext}<0.01T changes directional components distribution of total

magnetic moment of Er ions (compare fig.28 and fig. 29).

Similar behavior of magnetic moment directions was reported in ref. [7], but most of the presented results of calculations of properties of $ErAl_2$ still await experimental verification.

5 Conclusions

We performed calculations for $HoAl_2$ and $ErAl_2$ thermomagnetic properties using the ATOMIC MATTERS MFA computation system. The local symmetry of the Ho and Er ions is cubic, which significantly simplifies the analyses. All the calculations were performed without free parameters. Very good agreement was obtained between thermomagnetic properties and experimental data. This confirms the effectiveness of our theoretical approach. Working with ATOMIC MATTERS MFA revealed its high usefulness. The visual form of calculationresults, full 3D interactive CEF potential visualization, intuitive tools for convention and unit recalculation, and the ability to compare data results all allow the user to utilize the power of the application very effectively. In conclusion, we confirm that ATOMIC MATTERS MFA is a unique application that combines a package of tools for correctly describing the physical properties of atomic-like electron systems subjected to electromagnetic interactions in real materials. This is an accurate tool for calculating properties of ions under the influence of the electrostatic potential of definable symmetry and both external and inter-ionic magnetic fields taken as a mean field approximation in magnetically ordered state.

This paper is the third in a series devoted to the RAl_2 (R=rare earth) compounds family. The same set of parameters is used for heavy rare earth elements: Dy, Tb, Tm and Gd in this crystal structure in two parallel papers.

References:

[1] Rafał Michalski, Jakub Zygadło. *Describing the Fine Electronic Structure and Predicting Properties of Materials with ATOMIC MATTERS Computation System*. Proceedings: 18th Int. Conf. on Physics, Mathematics and Computer Science - Dubai UE 01.06.2016. http://waset.org/publications/10004653/pdf.

[2] Rafał Michalski, Jakub Zygadło, *Thermal dependences of single ionic, magnetic properties of materials in ordered state, calculated with ATOMIC MATTERS MFA computation system*– Poceedengs: 7th IIF-IIR International Conference on Magnetic Refrigeration at Room Temperature, **Thermag VII** - Torino ITALY, 11-14 September 2016. – in printing

[3] H.G. Purwins and A. Leson, *Adv. Phys.* **39** (1990) 309.

[4] L.A. Gil, J.C.P. Campoy, E.J.R. Plaza and M.V. de Souza, *Journal of Magnetism and Magnetic Materials* 409 (2016) 45–49.

[5] *Magnetic and magnetoresistive properties of cubic Laves phase $HoAl_2$ single crystal*, M. Patra, S. Majumdar and S. Giri, Y. Xiao, T. Chatterji (2011) **arXiv:1107.1975 [cond-mat.mtrl-sci]**

[6] F. W. Wang, X. X. Zhang, and F. X. Hu, *Appl. Phys. Lett.*, Vol. **77**, No. 9 (2000)1360.

[7] P.O.Ribeiro, B.P.Alho, T.S.T.Alvarenga, E.P.Nóbrega, V.S.R.deSousa, A.Magnus G.Carvalho, A.Caldas, N.A.deOliveira, P.J.vonRanke, *Journal of Magn. Magn. Mater.* **379** (2015) 112–116.

[8] P.Wikusa, E.Canavan, S.T.Heine, K.Matsumoto, T.Numazawa *Cryogenics Preprint* (2014)

[9] Software website: www.atomicmatters.eu

[10] C. Rudowicz, C. Y Chung, *The generalization of the extended Stevens operators, J. Phys.: Condens. Matter* **16** (2004) 5825–5847.

[11] P.G.de Gennes *J.Phys.Radiat* **23** (1962) 5010.

[12] M. T. Hutchings, Solid State Phys. **16** (New York (1964) 227.

[13] B. G. Wybourne, *Symmetry Principles and Atomic Spectroscopy*, J. Wiley and Sons, New York (1970).

[14] A. Abragam and B. Bleaney, *EPR of Transition Ions*, Clarendon Press, Oxford (1970).